Distance statistics in large toroidal maps

E. Guitter

Institut de Physique Théorique
CEA, IPhT, F-91191 Gif-sur-Yvette, France
CNRS, URA 2306
emmanuel.guitter@cea.fr

Abstract

We compute a number of distance-dependent universal scaling functions characterizing the distance statistics of large maps of genus one. In particular, we obtain explicitly the probability distribution for the length of the shortest non-contractible loop passing via a random point in the map, and that for the distance between two random points. Our results are derived in the context of bipartite toroidal quadrangulations, using their coding by well-labeled 1-trees, which are maps of genus one with a single face and appropriate integer vertex labels. Within this framework, the distributions above are simply obtained as scaling limits of appropriate generating functions for well-labeled 1-trees, all expressible in terms of a small number of basic scaling functions for well-labeled plane trees.

1. Introduction

The understanding of random maps is a fundamental issue in combinatorics and many map enumeration results were obtained over the years, using for instance recursive decomposition [1], matrix integrals [2, 3] or bijective methods [4-6]. Of particular interest in the scaling limit of large random maps, which converge toward nice universal probabilistic objects whose metric properties are only partially understood. This limit is especially relevant to physics, where maps are used as discrete models for fluctuating surfaces, e.g. in the field of biological membranes or that of string theory. In physics, maps are often equipped with statistical models, such as spins or particles, presenting a large variety of critical phenomena. This gives rise to many possible sensible scaling limits of continuous surfaces, each defining a particular universality class of maps. Their classification and characterization are the aim of the so-called two-dimensional quantum gravity [7,8].

The simplest universality class is that of the so-called pure gravity, which describes the scaling limit of large maps with prescribed face degrees, such as triangulations (maps with faces of degree 3 only) or quadrangulations (maps with faces of degree 4 only), possibly equipped with non-critical statistical models. In this universality class,

a particular attention was payed to the limit of large *planar* maps, i.e. maps with the topology of the two-dimensional sphere, converging to the so-called Brownian map [9,10].

Even if its topology remains that of a sphere [11,12], the Brownian map presents nevertheless intriguing metric properties such as a remarkable phenomenon of confluence of its geodesics [13], which reveals an underlying tree-like structure. More quantitatively, the geometry of the Brownian map was characterized by a number of distributions measuring its distance statistics, such as its two-point function [14-17], which is the law for the distance between two random points in the map and its three-point function [18], which is the joint law for the three mutual distances between three points. Other refined distributions, measuring e.g. the length of "separating loops" or that of the common part of confluent geodesics, were also obtained [19]. Beside the spherical topology, the case of maps with a single boundary was also considered [20], with an explicit derivation of the law for the distance of a random point to the boundary.

The most advanced results on the distance statistics in maps were obtained in the context of planar quadrangulations, using a bijection by Schaeffer [5] which gives a coding for these maps by so-called *well-labeled trees*, i.e. plane trees whose vertices carry integer labels with particular constraints. This approach turned out to be the most adapted to address distance-related question since the labels precisely encode some of the distances in the original map. An extension of the Schaeffer bijection was also found by Marcus and Schaeffer [21-22], which establishes a bijection between bipartite quadrangulations of arbitrary genus h and so-called *well-labeled h-trees*, which are maps of genus h with one face only, and whose vertices carry integer labels with the same constraints as in the planar case. In view of this result, a very natural question is therefore that of the distance statistics in maps of arbitrary genus. The Marcus-Schaeffer bijection was used very recently [23] to discuss the scaling limit of large bipartite quadrangulations of fixed genus, showing in particular the convergence to a limiting object with Hausdorff dimension 4, yet to be characterized.

The purpose of this paper is precisely to give a quantitative characterization of the distance statistics in large toroidal maps, i.e. maps of genus 1. We will in particular derive an explicit expression for the two-point function of large toroidal maps, which differs from that of the planar case. In the case of genus 1, we may also define a non-trivial "one-point function" by measuring the length of the shortest *non-contractible* loop passing via a given point. We give here the corresponding limiting probability distribution for large maps. These results are obtained again in the simplest context of genus 1 bipartite quadrangulations, using the Marcus-Schaeffer bijection above with well-labeled 1-trees.

The paper is organized as follows: in Section 2, we present our basic tools which are a number generating functions for well-labeled (plane) trees with marked vertices, with a particular emphasis on their scaling limit. We then recall in Section 3 the Marcus-Schaeffer bijection between pointed (i.e. with a marked vertex called the origin) bipartite quadrangulations of genus h and well-labeled h-trees. As an exercise, we show how to recover the number of genus 1 bipartite quadrangulations from our basic generating functions of Section 2. We then compute in Section 4 two different one-point

functions for large pointed toroidal maps: the probability distribution for the length of the shortest non-contractible loop passing via the origin of the map and that for the length of the "second-shortest" loop, which is the shortest among non-contractible loops not homotopic to the shortest non-contractible one (or its powers). We finally derive in Section 5 the expression for the two-point function of large toroidal maps, which is the law for the distance from the origin of a random point in the map. We gather a few concluding remarks in Section 6.

2. Basic tools: generating functions for well-labeled trees

In this section, we recall a number of known expressions for generating functions of *well-labeled trees* and derive a few new ones. As will be apparent later, the explicit formulas displayed here will serve as basic tools to obtain, in the next sections, various distance related generating functions in ensembles of large toroidal maps.

By well-labeled tree, we mean a plane tree whose vertices carry integer labels such that:

(i) the labels on two vertices adjacent in the tree differ by at most 1;

(ii) the minimum label is 1.

It is useful to also introduce almost well-labeled trees where (ii) is replaced by the weaker condition:

(ii)' all labels are larger than or equal to 1.

The first generating function of interest is that, $R_\ell \equiv R_\ell(g)$, of *planted* almost well-labeled trees, with a weight g per edge, and with root label ℓ ($\ell \geq 1$). It was computed in [17], with the result:

$$\begin{aligned} R_\ell &= R\,\frac{(1-x^\ell)(1-x^{\ell+3})}{(1-x^{\ell+1})(1-x^{\ell+2})} \\ \text{with } R &= \frac{1-\sqrt{1-12g}}{6g} \quad \text{and } x+\frac{1}{x}+1=\frac{1}{gR^2}\ . \end{aligned} \tag{2.1}$$

This particular form is obtained by solving of the recursion relation

$$R_\ell = \frac{1}{1-g(R_{\ell+1}+R_\ell+R_{\ell-1})}\ , \tag{2.2}$$

with initial condition $R_0 = 0$, expressing that an almost well-labeled tree with root label ℓ is coded by the sequence of its descending subtrees, themselves almost well-labeled trees with root label ℓ or $\ell \pm 1$.

The contribution to R_ℓ of large trees is encoded in the behavior of this generating function in the vicinity of the critical point $g = 1/12$. Setting

$$g = \frac{1}{12}(1-\epsilon^2) \tag{2.3}$$

with $\epsilon \to 0$, a non-trivial scaling limit is reached for R_ℓ by letting ℓ become large as

$$\ell = \frac{L}{\sqrt{\epsilon}} \tag{2.4}$$

with L finite. In this limit, we have the expansion

$$\begin{aligned} R_\ell &= 2\left(1 - \epsilon\,\mathcal{F}(L) + \mathcal{O}(\epsilon^{3/2})\right) \\ \text{with } \mathcal{F}(L) &= 1 + \frac{3}{\sinh^2\left(\sqrt{\frac{3}{2}}L\right)}\ . \end{aligned} \tag{2.5}$$

The scaling function $\mathcal{F}$ satisfies the non-linear differential equation

$$\mathcal{F}'' = 3(\mathcal{F}^2 - 1) \tag{2.6}$$

which is the continuous counterpart of eq. (2.2), obtained by expanding this discrete equation at order ϵ^2.

Another basic generating function is that, X_ℓ ($\ell \geq 1$), of almost well-labeled trees with *two distinct* (and distinguished) *marked vertices carrying the same label* ℓ and such that the labels on the (unique) shortest path in the tree joining these two vertices are all larger than or equal to ℓ. Adding for convenience a trivial contribution 1 to X_ℓ, we have the recursion relation

$$X_\ell = 1 + gR_\ell^2 X_\ell (1 + gR_{\ell+1}^2 X_{\ell+1}) \tag{2.7}$$

obtained by inspecting the first occurrence of a label ℓ on the shortest path joining the two marked vertices. The solution of (2.7) reads

$$X_\ell = \frac{(1-x^3)(1-x^{\ell+1})^2(1-x^{2\ell+3})}{(1-x)(1-x^{\ell+3})^2(1-x^{2\ell+1})} \tag{2.8}$$

with x as above. In the scaling limit, we have the expansion

$$\begin{aligned} X_\ell &= 3\left(1 - \sqrt{\epsilon}\,\mathcal{C}(L) + \mathcal{O}(\epsilon)\right) \\ \text{with } \mathcal{C}(L) &= \sqrt{6}\ \frac{2 + \cosh(\sqrt{6}L)}{\sinh(\sqrt{6}L)} \end{aligned} \tag{2.9}$$

while eq. (2.7), expanded at leading order in ϵ, translates into

$$\mathcal{C}' = \mathcal{C}^2 - 6\mathcal{F}\ . \tag{2.10}$$

From the explicit forms of $\mathcal{F}$ and $\mathcal{C}$ above, we observe that me may write the identity

$$\mathcal{C} = -\frac{\mathcal{F}''}{\mathcal{F}'} = -\big(\log(-\mathcal{F}')\big)' \tag{2.11}$$

since $|\mathcal{F}'(L)| = -\mathcal{F}'(L)$ for real L. In this form, the relation (2.10) is a direct consequence of the relation (2.6).

A third useful generating function is that, $\tilde{X}_{\ell_1,\ell_2}$ ($\ell_1 > \ell_2 \geq 1$), of almost well-labeled trees with *two distinct* (and distinguished) *marked vertices carrying respective labels* ℓ_1 *and* ℓ_2, and such that labels on the (unique) shortest path in the tree joining them are all strictly larger than ℓ_2 (except of course at the endpoint of the path with label ℓ_2). By cutting this shortest path at the first occurrence of a label $\ell_1 - 1, \ell_1 - 2, \cdots$, we may write

$$\begin{aligned} \tilde{X}_{\ell_1,\ell_2} &= \prod_{\ell=\ell_2}^{\ell_1-1} g R_\ell R_{\ell+1} X_{\ell+1} \\ &= x^{\ell_1-\ell_2} \frac{(1-x^{\ell_2})(1-x^{\ell_2+1})(1-x^{\ell_2+2})(1-x^{\ell_2+3})(1-x^{2\ell_1+3})}{(1-x^{\ell_1})(1-x^{\ell_1+1})(1-x^{\ell_1+2})(1-x^{\ell_1+3})(1-x^{2\ell_2+3})} \, . \end{aligned} \tag{2.12}$$

This last expression is extended to the case $\ell_1 = \ell_2$ by adopting the convention that $\tilde{X}_{\ell_2,\ell_2} = 1$. In the scaling limit, setting $\ell_1 = L_1/\sqrt{\epsilon}$ and $\ell_2 = L_2/\sqrt{\epsilon}$, we have the expansion

$$\begin{aligned} &\tilde{X}_{\ell_1,\ell_2} = \tilde{\mathcal{C}}(L_1, L_2) + \mathcal{O}(\sqrt{\epsilon}) \\ &\text{with } \tilde{\mathcal{C}}(L_1, L_2) = \frac{\cosh\left(\sqrt{\frac{3}{2}} L_1\right) \sinh^3\left(\sqrt{\frac{3}{2}} L_2\right)}{\cosh\left(\sqrt{\frac{3}{2}} L_2\right) \sinh^3\left(\sqrt{\frac{3}{2}} L_1\right)} \, . \end{aligned} \tag{2.13}$$

Note that this expression can be obtained alternatively by looking at the continuous counterpart of the product formula in (2.12). Indeed, using $g R_\ell R_{\ell+1} X_{\ell+1} \sim (1/12) \times 2^2 \times 3 \, (1 - \sqrt{\epsilon}\, \mathcal{C}(L))$, we may write directly

$$\tilde{\mathcal{C}}(L_1, L_2) = \exp\left(- \int_{L_2}^{L_1} \mathcal{C}(L) \, dL \right) = \exp\left(- \big[- \log(-\mathcal{F}') \big]_{L_2}^{L_1} \right) = \frac{\mathcal{F}'(L_1)}{\mathcal{F}'(L_2)} \tag{2.14}$$

which matches (2.13).

The final important quantity is what we shall call the "propagator", which is the generating function K_{ℓ_1,ℓ_2} ($\ell_1, \ell_2 \geq 1$) of almost well-labeled trees with *two distinct* (and distinguished) *marked vertices with respective labels* ℓ_1 *and* ℓ_2, and with no additional condition on the labels in-between (apart of course from the general conditions (i) and (ii)' of almost well-labeled trees). This generating function reads

$$K_{\ell_1,\ell_2} = -\delta_{\ell_1,\ell_2} + \sum_{\ell=1}^{\min(\ell_1,\ell_2)} \tilde{X}_{\ell_1,\ell} \tilde{X}_{\ell_2,\ell} X_\ell \tag{2.15}$$

as obtained by summing over the minimum label ℓ on the path joining the two marked vertices. Note that we insist here on the two marked vertices being distinct, with a path

of non-zero length in-between and that, if $\ell_1 = \ell_2$, we have to subtract an undesired contribution 1 in the sum. The generating function K_{ℓ_1,ℓ_2} is solution of the equation

$$K_{\ell_1,\ell_2} = gR_{\ell_1}\Big(R_{\ell_1+1}(\delta_{\ell_1+1,\ell_2} + K_{\ell_1+1,\ell_2}) + R_{\ell_1}(\delta_{\ell_1,\ell_2} + K_{\ell_1,\ell_2}) + R_{\ell_1-1}(\delta_{\ell_1-1,\ell_2} + K_{\ell_1-1,\ell_2})\Big) \tag{2.16}$$

with $K_{0,\ell_2} = 0$, obtained by looking at the label $\ell_1, \ell_1 \pm 1$ of the vertex adjacent to the first marked vertex on the path joining the two marked vertices. We have no compact formula for K_{ℓ_1,ℓ_2} at the discrete level but, in the scaling limit, eq. (2.15) translates into the expansion

$$\begin{aligned} &K_{\ell_1,\ell_2} = \frac{\rho(L_1,L_2)}{\sqrt{\epsilon}} + \mathcal{O}(1) \\ &\text{with } \rho(L_1,L_2) = \int_0^{\min(L_1,L_2)} 3\,\tilde{\mathcal{C}}(L_1,L)\tilde{\mathcal{C}}(L_2,L)\,dL \end{aligned} \tag{2.17}$$

with a simple factor 3 for the limit of X_ℓ. Using (2.14), we may now compute the integral and write a compact expression for $\rho(L_1, L_2)$:

$$\begin{aligned} &\rho(L_1,L_2) = \mathcal{F}'(L_1)\mathcal{F}'(L_2) \times \mathcal{H}\big(\min(L_1,L_2)\big) \\ &\text{where } \mathcal{H}(L) = \frac{1}{2^6 3^3}\left(180L + \sqrt{6}\left(\sinh\left(2\sqrt{6}L\right) - 16\sinh\left(\sqrt{6}L\right) - 32\tanh\left(\sqrt{\frac{3}{2}}L\right)\right)\right). \end{aligned} \tag{2.18}$$

Note that the somewhat involved function $\mathcal{H}(L)$ is simply characterized by

$$\mathcal{H}'(L) = \frac{3}{\big(\mathcal{F}'(L)\big)^2} \tag{2.19}$$

with $\mathcal{H}(0) = 0$. It is a straightforward exercise to check that the continuous propagator $\rho(L_1, L_2)$ above is solution of the equation

$$\frac{\partial^2}{\partial L_1^2}\rho(L_1,L_2) = 6\mathcal{F}(L_1)\rho(L_1,L_2) - 3\,\delta(L_1 - L_2) \tag{2.20}$$

which is the continuous counterpart of (2.16). Up to a (somewhat arbitrary) global normalization of the coordinate L, this is precisely the equation satisfied by the two-point function of a polymer chain embedded in one dimension (with coordinate L) subject to a potential $V(L) \propto \mathcal{F}(L) - 1 \propto 1/\sinh^2(\sqrt{3/2}L)$. Heuristically, this polymer corresponds to the (unique) path between the two marked points in the tree and its configuration in one-dimensional space simply reproduces the sequence of labels along this path. From condition (ii)', the presence of the other attached subtrees exerts on the polymer an effective repulsion from the position $L = 0$ encoded in the potential $V(L)$.

When $\ell_1 \to \infty$, $K_{\ell_1,\ell_2} \to 0$ unless we also send $\ell_2 \to \infty$, keeping $p \equiv \ell_2 - \ell_1$ finite. Defining

$$k_p \equiv \lim_{\ell_1 \to \infty} K_{\ell_1,\ell_1+p} \ , \tag{2.21}$$

for an arbitrary integer p, this quantity satisfies the equation

$$k_p = g\, R^2 (k_{p-1} + k_p + k_{p+1} + \delta_{p,1} + \delta_{p,0} + \delta_{p,-1}) \tag{2.22}$$

and we find explicitly

$$k_p = \frac{1-x^3}{(1-x)(1-x^2)}\, x^{|p|} - \delta_{p,0} \tag{2.23}$$

with x as in (2.1). In the scaling limit, and for large values of L_1 and L_2, we have the corresponding limiting behavior

$$\rho(L_1, L_2) \sim \frac{\sqrt{6}}{4} \exp(-\sqrt{6}\, |L_1 - L_2|) \tag{2.24}$$

where we recognize the usual (translation invariant) two-point function for a polymer in one dimension without potential.

The above quantities X_ℓ, $\tilde{X}_{\ell_1,\ell_2}$ and K_{ℓ_1,ℓ_2} may alternatively be viewed as generating functions for *chains* of almost well-labeled trees, with endpoints carrying prescribed labels. In the following, we will consider various generating functions for more involved well-labeled structures coding for toroidal maps. At the discrete level, those are naturally formed of a number of chains as above, attached by their endpoints. The knowledge of the scaling forms $\mathcal{C}(L)$, $\tilde{\mathcal{C}}(L_1, L_2)$ and $\rho(L_1, L_2)$ for the chain generating functions will be sufficient to derive explicit expressions for the scaling form of these more involved toroidal generating functions. This eventually will translate into explicit universal scaling functions characterizing the distance statistics of large toroidal maps.

3. The Marcus-Schaeffer bijection for bipartite quadrangulations of genus 1

Our approach on the distance statistics of large toroidal maps relies on the bijection by Marcus and Schaeffer between, one the one hand, *pointed bipartite quadrangulations of fixed genus h* and on the other hand, *well-labeled h-trees*. By pointed bipartite quadrangulation, we mean a map whose faces all have degree 4 (quadrangulation), whose vertices can be colored in black and white in such a way that adjacent vertices have a different color (bipartite) and with a marked vertex called the origin (pointed). It was shown by Marcus and Schaeffer [21] that any such map of genus h is bijectively coded by a well-labeled h-tree, i.e. a map of genus h with exactly one face (h-tree) and whose vertices carry integer labels subject to the two conditions (i) and (ii) of section 2 (well-labeled). As before, it is convenient to also introduce the notion of almost well-labeled h-tree where condition (ii) is replaced by the weaker condition (ii)'.

Note that a quadrangulation with n faces and genus h has $2n$ edges and $n+2-2h$ vertices. The n faces of the quadrangulation are in one-to-one correspondence with the

edges of the well-labeled h-tree, which therefore has n edges and $n+1-2h$ vertices. These $n+1-2h$ vertices are in one-to-one correspondence with the $(n+2-2h)-1$ vertices of the quadrangulation other than its origin, and the label of a vertex in the h-tree is nothing but the *distance from the associated vertex to the origin* in the quadrangulation. Finally, the $2n$ corners of the h-tree (i.e. the angular sectors between consecutive edges around a vertex) are in one-to-one correspondence with the $2n$ edges of the quadrangulation. More precisely, the corners with label ℓ (i.e. around a vertex with label ℓ) in the h-tree are in one-to-one correspondence with the edges of type $(\ell-1) \to \ell$ in the quadrangulation, i.e. the edges connecting a vertex at distance $(\ell-1)$ from the origin to a vertex at distance ℓ.

It is useful to recall how to recover the quadrangulation from its well-labeled h-tree coding. For the vertices of the quadrangulation, we take all the vertices of the h-tree plus an extra vertex added inside its unique face. This vertex will be the origin of the (pointed) quadrangulation. The edges of the quadrangulation are obtained by *linking each corner with label ℓ in the h-tree to its successor*, which is the added vertex for $\ell = 1$ and, for $\ell > 1$, the first corner with label $\ell-1$ encountered, say counterclockwise around the unique face of the h-tree. These links can be drawn without mutual crossings inside the face of the h-tree and, by construction, they do not intersect the original edges of this h-tree. Note that the sequence of links between the successive successors of a given corner with label ℓ provides a particular geodesic (i.e. shortest) path of length ℓ in the quadrangulation, leading from the vertex underlying this corner to the origin vertex. After drawing the quadrangulation edges, we may erase all the original edges of the h-tree as well as all the labels. Note that the obtained quadrangulation is automatically bipartite.

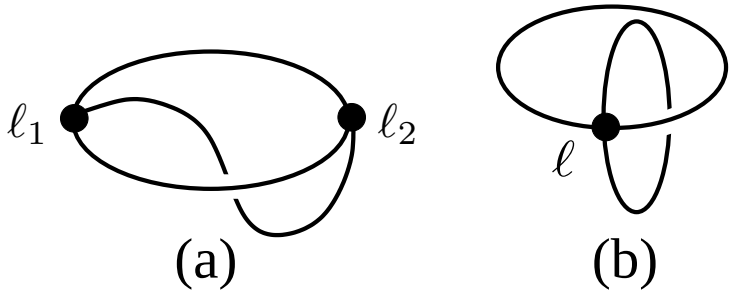

Fig. 1: The two possible backbones for 1-trees: (a) a generic backbone with two vertices of degree 3 carrying positive labels ℓ_1 and ℓ_2 linked by three edges and (b) a degenerate backbone with one vertex of degree 4 with positive label ℓ, linked to itself by two edges.

In the spherical case $h = 0$, the well-labeled 0-trees are nothing but the well-labeled trees of Section 2, so that our generating functions above translate into generating functions for pointed quadrangulations (note that we need not specify that the quadrangulation is bipartite since this is automatic for $h = 0$). For instance, choosing a corner with label ℓ in a well-labeled tree amounts to picking an edge at distance ℓ from the

origin (i.e. an edge of type $(\ell-1)\to\ell$) in the associated quadrangulation. The generating function for pointed planar quadrangulations with a marked edge at distance ℓ is therefore that of planted well-labeled trees with root label ℓ. It is given by $R_\ell - R_{\ell-1}$ since we have to subtract from R_ℓ those configurations with minimum label larger than or equal to 2. These undesired configurations correspond exactly to almost well-labeled configurations having all their labels shifted by 1, hence they are counted by $R_{\ell-1}$. We will use the same shift argument in the following to transform generating functions for almost well-labeled objects into generating functions for their well-labeled analogs. For instance, the generating function for pointed planar quadrangulations with two marked distinct (and distinguished) vertices at distance ℓ_1 and ℓ_2 from the origin is given by $K_{\ell_1,\ell_2} - K_{\ell_1-1,\ell_2-1}$ in terms of the propagator.

In this paper, we focus on the case $h=1$ of toroidal topology. Well-labeled and almost well-labeled 1-trees may be classified according to their *backbone* obtained as follows: we first delete recursively each vertex with degree 1 and its incident edge until no degree 1 vertex is left in the 1-tree. The resulting object is an almost well-labeled 1-tree whose vertices all have degree larger than or equal to 2 by construction. We call this 1-tree the *skeleton* of the original 1-tree. We may then erase each vertex of degree 2 in the skeleton and concatenate the two incident edges, leading to a labeled 1-tree with vertices of degree larger than or equal to 3 and with arbitrary positive vertex labels. We call this 1-tree the *backbone* of the original 1-tree. From the Euler relation for maps, it is easily seen that only two types of backbones are possible:

(a) generic backbones, made of two 3-valent vertices with labels $\ell_1\geq\ell_2\geq 1$, linked by three edges (see figure 1-(a));
(b) degenerate backbones, made of a unique 4-valent vertex with label $\ell\geq 1$ linked to itself by two edges (see figure 1-(b)).

To obtain all the almost well-labeled 1-trees leading to a generic backbone, we simply have to replace each of the three edges of this backbone by an arbitrary non-empty chain of almost well-labeled trees with endpoints labeled by ℓ_1 and ℓ_2, as counted by the propagator K_{ℓ_1,ℓ_2}. The corresponding generating function reads therefore

$$\begin{array}{ll} \dfrac{1}{3}K^3_{\ell_1,\ell_2} & \text{if } \ell_1>\ell_2 \\ \dfrac{1}{6}K^3_{\ell_1,\ell_1} & \text{if } \ell_1=\ell_2\ . \end{array} \tag{3.1}$$

Here a factor $1/3$ is necessary to avoid over-counting as, in the sum, we recover 3 times the same configuration upon permuting cyclically the three edges of the skeleton. Similarly, an extra $1/2$ factor is necessary to balance the possibility of recovering the same configuration by exchanging the two vertices of degree 3 if they have the same label. This simple over-counting argument does not hold for configurations presenting a symmetry and these configurations are therefore enumerated in (3.1) with an inverse symmetry factor, which is a customary statistics. Note that the symmetric configurations are expected to become negligible for maps of large size n so that the symmetry factors have no effect on the scaling limit that we will discuss.

If we wish to keep only the well-labeled 1-trees, we have to remove those configurations for which the minimum label is larger than or equal to 2 and, using the same shift argument as above, we now get a generating function

$$\begin{array}{ll} \frac{1}{3}\left(K^3_{\ell_1,\ell_2}-K^3_{\ell_1-1,\ell_2-1}\right) & \text{if } \ell_1>\ell_2 \\ \frac{1}{6}\left(K^3_{\ell_1,\ell_1}-K^3_{\ell_1-1,\ell_1-1}\right) & \text{if } \ell_1=\ell_2 \end{array} \tag{3.2}$$

with the convention $K_{\ell_1,0}=K_{0,0}=0$.

Summing first over the smallest label ℓ_2, then over the largest one ℓ_1, we get the total contribution W_1 of all 1-trees having a generic backbone

$$\begin{aligned} W_1 &= \sum_{\ell_1=1}^{\infty}\left\{\frac{1}{6}\left(K^3_{\ell_1,\ell_1}-K^3_{\ell_1-1,\ell_1-1}\right)+\frac{1}{3}\sum_{\ell_2=1}^{\ell_1-1}\left(K^3_{\ell_1,\ell_2}-K^3_{\ell_1-1,\ell_2-1}\right)\right\} \\ &= \sum_{\ell_1=1}^{\infty}\left\{\left(\frac{1}{6}K^3_{\ell_1,\ell_1}+\frac{1}{3}\sum_{\ell_2=1}^{\ell_1-1}K^3_{\ell_1,\ell_2}\right)-\left(\frac{1}{6}K^3_{\ell_1-1,\ell_1-1}+\frac{1}{3}\sum_{\ell_2=1}^{\ell_1-2}K^3_{\ell_1-1,\ell_2}\right)\right\} \\ &= \lim_{\ell_1\to\infty}\left\{\frac{1}{6}K^3_{\ell_1,\ell_1}+\frac{1}{3}\sum_{\ell_2<\ell_1}K^3_{\ell_1,\ell_2}\right\} \\ &= \frac{1}{6}k_0^3+\frac{1}{3}\sum_{p<0}k_p^3=\frac{x^3(1+2x+2x^2-2x^3)}{2(1-x)^4(1+x)^2}\ . \end{aligned} \tag{3.3}$$

Similarly, the total contribution W_2 of all well-labeled 1-trees having a degenerate backbone is

$$\begin{aligned} W_2 &= \sum_{\ell_1=1}^{\infty}\frac{1}{4}\left(K^2_{\ell_1,\ell_1}-K^2_{\ell_1-1,\ell_1-1}\right) \\ &= \lim_{\ell_1\to\infty}\frac{1}{4}K^2_{\ell_1,\ell_1} \\ &= \frac{1}{4}k_0^2=\frac{x^2(1+2x)^2}{4(1-x)^2(1+x)^2}\ . \end{aligned} \tag{3.4}$$

Summing (3.3) and (3.4), we get the generating function for well-labeled 1-trees which, from the Marcus-Schaeffer bijection is also that, $Q^{(1)}_\bullet(g)$ of pointed bipartite quadrangulations of genus 1

$$Q^{(1)}_\bullet=W_1+W_2=\frac{x^2(1+4x+x^2)}{4(1-x)^4(1+x)^2}\ . \tag{3.5}$$

Note that the symmetry factor of a well-labeled 1-tree is also that of the associated pointed quadrangulation so that symmetric pointed quadrangulations are counted in $Q^{(1)}_\bullet$ with their usual inverse symmetry factor. It is more customary to consider *rooted*

maps, i.e. maps with a marked oriented edge, as they do not involve symmetry factors. The generating function for rooted bipartite quadrangulations of genus 1 is simply

$$Q_{\rightarrow}^{(1)} = 4Q_{\bullet}^{(1)} \tag{3.6}$$

since there are exactly twice as many edges as vertices in a genus 1 quadrangulation, each coming with two orientations. All the enumeration formulas above are consistent with those found in ref. [22].

If we are interested only in large maps, we can use the continuous analogs of (3.3) and (3.4) giving the leading singularity of W_1 and W_2, namely

$$\begin{aligned} W_1 &\sim \frac{1}{\epsilon^2} \lim_{L_1\to\infty} \frac{1}{3}\int_0^{L_1} dL_2\, \rho^3(L_1,L_2) \\ &= \frac{1}{3\epsilon^2}\int_{-\infty}^{0} dP \left(\frac{\sqrt{6}}{4}\right)^3 \exp(-3\sqrt{6}\,|P|) = \frac{1}{96\epsilon^2} \\ W_2 &\sim \frac{1}{\epsilon}\lim_{L_1\to\infty}\frac{1}{4}\rho^2(L_1,L_1) = \frac{1}{4\epsilon}\left(\frac{\sqrt{6}}{4}\right)^2 = \frac{3}{32\epsilon} \end{aligned} \tag{3.7}$$

which can also be directly read off (3.3) and (3.4) with $x \sim \exp(-\sqrt{6\,\epsilon})$. Note that the degenerate case is less singular than the generic case so that the dominant singularity of $Q_{\bullet}^{(1)}$ or $Q_{\rightarrow}^{(1)}$ comes from W_1 only.

Alternatively, we deduce from (3.7) the large n behavior of the number of well-labeled 1-trees with n edges having a generic or degenerate backbone

$$W_1|_{g^n} \sim \frac{12^n}{96}\ , \qquad W_2|_{g^n} \sim \frac{3\ 12^n}{32\sqrt{\pi n}}\ . \tag{3.8}$$

At large n, the dominant contribution to $Q_{\bullet}^{(1)}$ or $Q_{\rightarrow}^{(1)}$ comes from configurations with a generic backbone only and we recover the known asymptotics [22]

$$Q_{\rightarrow}^{(1)}|_{g^n} = 4Q_{\bullet}^{(1)}|_g^n \sim \frac{12^n}{24} \tag{3.9}$$

for the number of rooted bipartite quadrangulations of genus 1 with n faces.

4. One-point functions for large toroidal maps

For maps with a toroidal topology, we may define several interesting distance-dependent one-point functions. Starting with a pointed map, we may consider as a"self-distance" of the origin vertex the length of any shortest *non-contractible* loop in the map containing this origin. In the case of bipartite quadrangulations, we denote this length by 2ℓ as it is necessarily even. We may now use the coding of previous section and note

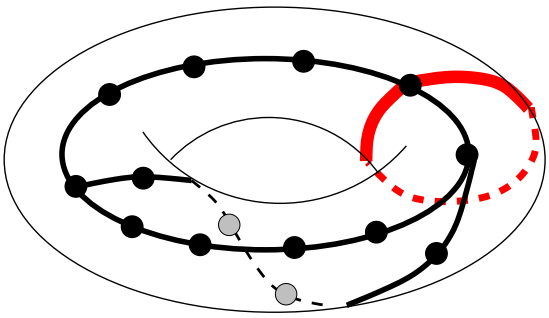

Fig. 2: A non-contractible loop (thick red) drawn on a toroidal quadrangulation must intersect the skeleton of the associated 1-tree at one of its vertices.

that any non-contractible loop in the quadrangulation must intersect the skeleton of the associated 1-tree. Now the edges of the quadrangulation lie strictly inside the unique face of the 1-tree and do not cross its edges so that the intersection with the skeleton necessarily takes place at one of the skeleton vertices, say with label ℓ' (see fig. 2 for an illustration). Since ℓ' is the distance in the quadrangulation from this vertex to the origin, the length of the loop is necessarily larger than or equal to $2\ell'$ so that the half-length ℓ of a shortest non-contractible loop is larger than or equal to the minimum label on the skeleton of the 1-tree. Picking now a vertex with minimal label $\ell_{\min}$ on this skeleton, this vertex has a degree larger than or equal to 2 by construction and we may consider two distinct corners around it. The two sequences of links between the successive successors of these corners define two paths of lengths $\ell_{\min}$ leading to the origin, which *do not intersect the skeleton* and whose concatenation therefore creates a non-contractible loop of length $2\ell_{\min}$. We deduce that

$$\ell = \ell_{\min}(\text{Sk.}) \tag{4.1}$$

where $\ell_{\min}(\text{Sk.})$ is the minimum label on the skeleton of the 1-tree coding for the pointed quadrangulation at hand.

In the scaling limit, as already noticed, it is sufficient to consider the contribution of configurations leading to a generic backbone and we denote by $\ell_1 = L_1/\sqrt{\epsilon}$ and $\ell_2 = L_2/\sqrt{\epsilon}$ the labels of its two vertices of degree 3, with $\ell_1 \geq \ell_2$, and by $m_1 = M_1/\sqrt{\epsilon}$, $m_2 = M_2/\sqrt{\epsilon}$ and $m_3 = M_3/\sqrt{\epsilon}$ the respective minimal labels on the three chains linking these vertices in the skeleton, with $m_1 \geq m_2 \geq m_3$ so that $\ell_{\min}(\text{Sk.}) = m_3$. With these notations, the generating function for almost well-labeled 1-tree whose skeleton has a

minimal label $\ell_{\min}(\text{Sk.}) = \ell = L\sqrt{\epsilon}$ behaves when $\epsilon \to 0$ as

$$\begin{aligned}
&\frac{2}{\epsilon^2}\int_{M_3}^{\infty} dM_2 \int_{M_2}^{\infty} dM_1 \int_{M_1}^{\infty} dL_2 \int_{L_2}^{\infty} dL_1 \; 3\,\tilde{\mathcal{C}}(L_1, M_1)\tilde{\mathcal{C}}(L_2, M_1) \times 3\,\tilde{\mathcal{C}}(L_1, M_2)\tilde{\mathcal{C}}(L_2, M_2) \\
&\qquad\qquad \times 3\,\tilde{\mathcal{C}}(L_1, M_3)\tilde{\mathcal{C}}(L_2, M_3)\Big|_{M_3=L} \\
&= \frac{2}{\epsilon^2}\frac{3}{\mathcal{F}'(L)^2}\int_{L}^{\infty} dM_2 \frac{3}{\mathcal{F}'(M_2)^2}\int_{M_2}^{\infty} dM_1 \frac{3}{\mathcal{F}'(M_1)^2}\int_{M_1}^{\infty} dL_2 \mathcal{F}'(L_2)^3 \int_{L_2}^{\infty} dL_1 \mathcal{F}'(L_1)^3 \\
&= \frac{\mathcal{I}(L)}{\epsilon^2} \qquad \text{with} \quad \mathcal{I}(L) = \frac{1}{96}\tanh^4\left(\sqrt{\frac{3}{2}}L\right) \; .
\end{aligned} \tag{4.2}$$

Note, as in (2.17), the factors 3 for the limit of each of the discrete terms X_{m_1}, X_{m_2} and X_{m_3}. Note also the factor 2 accounting for the two possible order of appearance of the minima m_1, m_2 and m_3 when turning around say the vertex with larger label ℓ_1.

To return to well-labeled configurations, we note that, as an alternative to the shift argument used in Section 3, we may equivalently use the property that almost well-labeled 1-trees whose skeleton has a minimal label ℓ are in one-to-one correspondence with well-labeled 1-trees whose skeleton has a minimal label smaller than or equal to ℓ. This correspondence is obtained by now shifting all labels in the almost well-labeled 1-tree by a non-negative integer so that its global minimum label (in the whole 1-tree) becomes 1. From the Marcus-Schaeffer bijection, we deduce that (4.2) may alternatively be viewed as the $\epsilon \to 0$ leading behavior of the *generating function for pointed bipartite quadrangulations with a shortest non-contractible loop passing via the origin of (rescaled) length smaller than* $2L$.

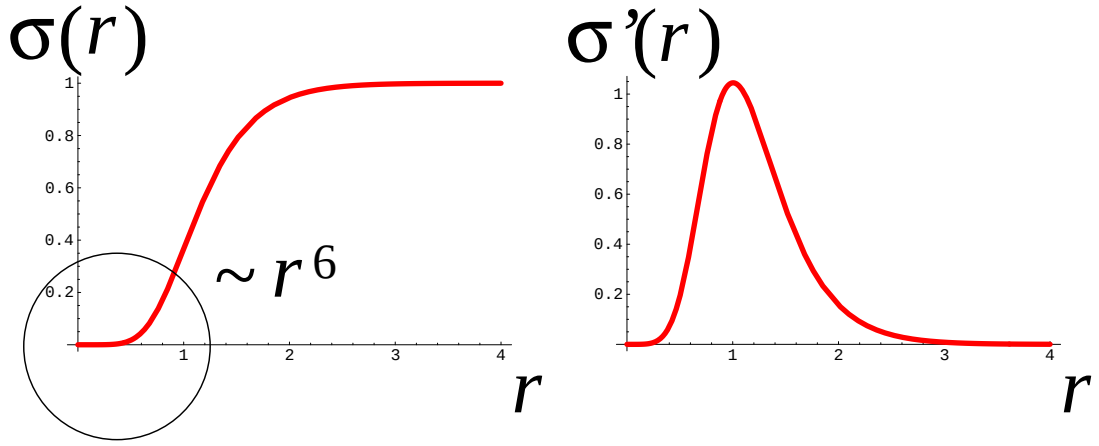

Fig. 3: Plots of the cumulative probability distribution $\sigma(r)$ and the associated probability density $\sigma'(r)$ for the rescaled half-length r of the shortest non-contractible loop passing via the origin of a large pointed toroidal quadrangulation.

From our one-point toroidal scaling function $\mathcal{I}(L)$, we may extract a (cumulative)

probability distribution in the ensemble of bipartite quadrangulations of genus 1 with fixed size n (= number of faces), in the limit of large n. At the discrete level, fixing the size amounts to picking the coefficient g^n in the generating function at hand, which can be done by a contour integral in g. In the limit of large n, this contour integral translates into an integral over a real variable ξ upon setting (see [17] for details)

$$g = \frac{1}{12}\left(1 + \frac{\xi^2}{n}\right) \ . \tag{4.3}$$

A sensible scaling limit is now obtained by rescaling ℓ as

$$\ell = r\, n^{1/4} \tag{4.4}$$

so that we can use in practice our continuous expressions above with $\epsilon = -\mathrm{i}\xi/\sqrt{n}$ and $L = \sqrt{-\mathrm{i}\xi}\, r$. Normalizing by $Q_\bullet^{(1)}|g^n$, we get the *probability*

$$\begin{aligned}\sigma(r) &= \frac{96}{\pi}\int_0^\infty d\xi\, \frac{1}{-\mathrm{i}\xi}\exp(-\xi^2)\left(\mathcal{I}(\sqrt{-\mathrm{i}\xi}r) - \mathcal{I}(\sqrt{\mathrm{i}\xi}r)\right) \\ &= \frac{8}{\pi}\int_0^\infty \frac{d\xi}{\xi}\exp(-\xi^2)\frac{\sin(\sqrt{3\xi}r)\sinh^3(\sqrt{3\xi}r) - \sinh(\sqrt{3\xi}r)\sin^3(\sqrt{3\xi}r)}{(\cosh(\sqrt{3\xi}r) - \cos(\sqrt{3\xi}r))^4}\end{aligned} \tag{4.5}$$

that the shortest non-contractible loop passing via the origin has a length smaller than $2rn^{1/4}$ *in the ensemble of pointed bipartite quadrangulations of genus* 1 *with fixed size* n, in the limit $n \to \infty$. The cumulative probability distribution $\sigma(r)$ and the associated probability density $\sigma'(r)$ are plotted in fig. 3. For small r, we have the expansion

$$\sigma(r) = \frac{9r^6}{4\sqrt{\pi}} - \frac{1431 r^{10}}{280\sqrt{\pi}} + \mathcal{O}(r^{14}) \ . \tag{4.6}$$

It is worth mentioning that, in the continuous limit, the shortest non-contractible loop is expected to be unique, i.e. two shortest loops at the discrete level remain at a distance negligible with respect to $n^{1/4}$ at large n. Moreover, as for geodesic paths in spherical maps, we expect a confluence phenomenon with the shortest loop made of an open part of (rescaled) length $2r - 2\delta$ and a common part of length δ traveled back and forth in the vicinity of the origin. The joint law for δ and r could be obtained in principle by a slight refinement of the above analysis.

In the same spirit, for a pointed map of genus 1, we may first consider a shortest non-contractible loop as above and now study the length of any shortest loop among those non-contractible loops *not homotopic to the shortest loop* or to any of its powers. A similar quantity was introduced in [24] an analyzed using heuristic scaling arguments. At the discrete level, this notion depends on the particular choice of the first shortest loop but we expect that this dependence is wiped out in the continuous limit in which the first shortest loop is essentially unique. We may as before assume that the well-labeled 1-tree coding for the quadrangulation has a generic backbone, i.e. has a skeleton

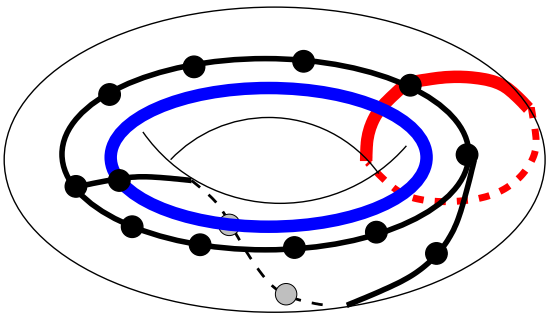

Fig. 4: Given a first non-contractible loop (thick red) intersecting only one of the three chains forming the skeleton, any other non-contractible loop non-homotopic to this first loop or to its powers (thick blue) must intersect (at least) one of the two other chains in the skeleton (possibly at an endpoint of the chain).

with two 3-valent vertices linked by three chains. We may moreover assume that the minimum label on this skeleton is reached for a bivalent vertex, i.e. strictly inside one of the three chains. Indeed, all the other situations (degenerate backbone or minimal label at one of the two 3-valent vertices of the skeleton) correspond to degenerate cases which give sub-dominant contributions in the continuous limit. We now take for the first loop the concatenation of the two sequences of links between the successive successors of the two corners at the above bivalent vertex with minimal label. A non-contractible loop not homotopic to this loop or to its powers must necessarily intersect the skeleton at one of the two other chains so that its length is larger than twice the label of any vertex of the skeleton minus the first chain (see fig. 4 for an illustration). Taking a vertex with minimal label $\ell_{\min}$ in this set, the two sequences of successors of two corners at this vertex, once concatenated, create a suitable loop of length $2\ell_{\min}$.

To summarize, denoting as before by L_1 and L_2 the (rescaled) labels of the 3-valent vertices of the skeleton, with $L_1 \geq L_2$, and by M_1, M_2 and M_3 the respective minimal labels on the three chains linking them, with $M_1 \geq M_2 \geq M_3$, the length we are now interested in is nothing but the second minimum M_2 so that, integrating over the other variables, we are now led to compute

$$\begin{aligned}
&\frac{2}{\epsilon^2}\int_0^{M_2} dM_3 \int_{M_2}^{\infty} dM_1 \int_{M_1}^{\infty} dL_2 \int_{L_2}^{\infty} dL_1 \; 3\,\tilde{\mathcal{C}}(L_1,M_1)\tilde{\mathcal{C}}(L_2,M_1) \times 3\,\tilde{\mathcal{C}}(L_1,M_2)\tilde{\mathcal{C}}(L_2,M_2) \\
&\qquad\qquad \times 3\,\tilde{\mathcal{C}}(L_1,M_3)\tilde{\mathcal{C}}(L_2,M_3)\Big|_{M_2=L} \\
&= \frac{2}{\epsilon^2}\frac{3}{\mathcal{F}'(L)^2}\int_0^{L} dM_3 \frac{3}{\mathcal{F}'(M_3)^2}\int_{L}^{\infty} dM_1 \frac{3}{\mathcal{F}'(M_1)^2}\int_{M_1}^{\infty} dL_2 \mathcal{F}'(L_2)^3 \int_{L_2}^{\infty} dL_1 \mathcal{F}'(L_1)^3 \\
&= \frac{\mathcal{J}(L)}{\epsilon^2} \qquad \text{with} \quad \mathcal{J}(L) = -\frac{1}{2}\mathcal{H}(L)\,\mathcal{F}'(2L)
\end{aligned} \tag{4.7}$$

with $\mathcal{H}$ as in (2.18).

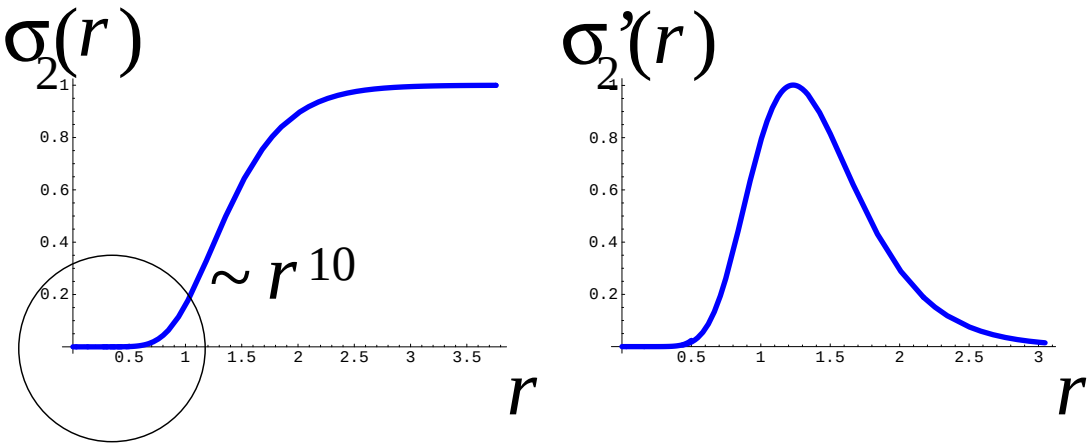

Fig. 5: Plots of the cumulative probability distribution $\sigma_2(r)$ and the associated probability density $\sigma_2'(r)$ for the rescaled half-length r of the "second shortest" non-contractible loop passing via the origin of a large pointed toroidal quadrangulation.

Repeating the above arguments, we get the *probability*

$$\sigma_2(r) = \frac{96}{\pi} \int_0^\infty d\xi \, \frac{1}{-\mathrm{i}\xi} \exp(-\xi^2) \left(\mathcal{J}(\sqrt{-\mathrm{i}\xi} r) - \mathcal{J}(\sqrt{\mathrm{i}\xi} r) \right) \tag{4.8}$$

that, in the set of all non-contractible loops passing via the origin, the "second shortest" loop, i.e. the shortest among loops not homotopic to any power of the true shortest one, has a length smaller than $2rn^{1/4}$ *in the ensemble of pointed bipartite quadrangulations of genus* 1 *with fixed size* n, in the limit $n \to \infty$. The cumulative probability distribution $\sigma_2(r)$ and the associated probability density $\sigma_2'(r)$ are plotted in fig. 5. For small r, we have the expansion

$$\sigma_2(r) = \frac{11043 \; r^{10}}{5096\sqrt{\pi}} + \mathcal{O}(r^{14}) \; . \tag{4.9}$$

It is interesting to comment on the small r behavior of both $\sigma(r)$ and $\sigma_2(r)$ which informs us on the regime of large but finite values of ℓ, namely: $1 \ll \ell \ll n^{1/4}$. For such a finite value of ℓ, the *average number of vertices* in a random quadrangulation giving rise to a shortest non-contractible loop of length smaller than 2ℓ scales as

$$n\sigma(r) \sim n \times r^6 = n \left(\frac{\ell}{n^{1/4}} \right)^6 = \frac{\ell^6}{\sqrt{n}} \tag{4.10}$$

where we dropped the multiplicative prefactor. In particular, this quantity tends to 0 as $n^{-1/2}$ for large n. This is to be contrasted with, for instance, the average number ($\propto n(\ell/n^{1/4})^4 = \ell^4$) of vertices at a finite distance less than ℓ from the origin of a pointed planar quadrangulation [17] which remains finite at large n. The explanation for this phenomenon is that a prerequisite for the shortest non-contractible loop passing

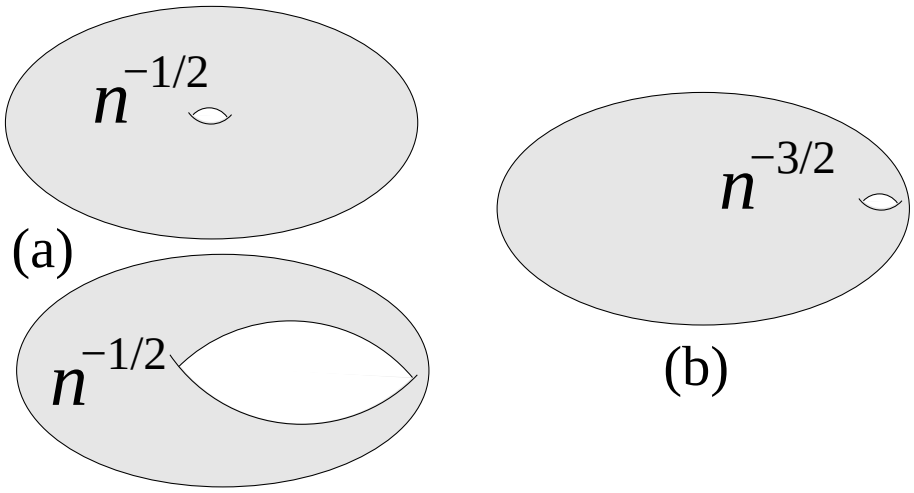

Fig. 6: A schematic picture of a toroidal quadrangulation with (a) a small non-contractible loop or (b) two non-homotopic small non-contractible loops. The first case occurs with a probability decaying as $n^{-1/2}$ and the second with a probability decaying as $n^{-3/2}$.

via the origin to be finite is that the smallest non-contractible loop in the map be itself finite, while (4.10) essentially counts the vertices lying at a finite distance from this non-contractible smallest loop. The n dependence in (4.10) is compatible with a probability of having a *finite* smallest non-contractible loop decaying as $n^{-1/2}$ in the set of bipartite quadrangulations of genus 1 and fixed large size n (see fig. 6-(a) for an illustration). Similarly, from the small r behavior of $\sigma_2(r)$, the number of vertices giving rise to a second-shortest loop of finite length smaller than 2ℓ behaves as

$$n\sigma_2(r) \sim n \times r^{10} = n \left(\frac{\ell}{n^{1/4}} \right)^{10} = \frac{\ell^{10}}{n^{3/2}} \ . \tag{4.11}$$

We now interpret the n dependence in (4.11) as measuring, in the set of bipartite quadrangulations with genus 1 and fixed size n, the probability that a quadrangulation has its two non-homotopic smallest non-contractible loops finite: this probability tends to 0 as $n^{-3/2}$ (see fig. 6-(b) for an illustration).

These scaling behaviors are not surprising since, in case (a) of fig. 6, the quadrangulation may essentially be viewed as a planar quadrangulation with two marked points which are glued together to create a handle, while in case (b), the quadrangulation is essentially a planar quadrangulation with one marked point. Recall that the number of planar quadrangulations of size n with a marked vertex is [1]

$$\frac{3^n}{2n} \frac{\binom{2n}{n}}{n+1} \sim \frac{12^n}{\sqrt{\pi} n^{5/2}} \tag{4.12}$$

while that with two marked vertices is (asymptotically) n times bigger. Dividing by the number of total number $Q^{(1)}_{\rightarrow}|_{g^n}/(4n) \sim 12^n/(96n)$ of quadrangulations of genus 1 gives a ratio scaling precisely as $n^{-1/2}$ for two marked points and $n^{-3/2}$ for one.

To summarize, we deduce a contrario that a generic bipartite quadrangulation of genus 1 has both its smallest cycles of order $n^{1/4}$ so that its topology remains that of a genus 1 surface in the scaling limit.

5. Two-point function for large toroidal maps

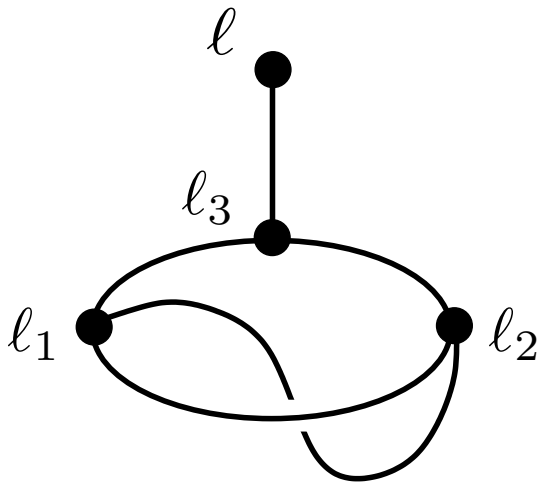

Fig. 7: The "diagram" enumerating generic configurations contributing to the dominant singularity of Z_ℓ. Each edge of the diagram must be replaced by a propagator K with the indices of its endpoints. We must then sum over ℓ_1, ℓ_2 and ℓ_3, keeping ℓ fixed.

The most natural measure of the distance statistics is via the two-point function which measures the density of points at a fixed distance from a given origin in the map. More precisely, we may decide to enumerate pointed bipartite quadrangulations of genus 1 with now *a marked vertex at distance ℓ ($\ell \geq 1$) from the origin*. From the Marcus-Schaeffer bijection, this amounts to enumerating well-labeled 1-trees with a marked vertex with label ℓ. As before, it is simpler to consider the generating function Z_ℓ for *almost* well-labeled 1-trees with a marked vertex with label ℓ. From the Marcus-Schaeffer bijection, Z_ℓ is now the generating function for pointed bipartite quadrangulations of genus 1 with a marked vertex at distance *less than or equal to* ℓ.

The dominant singularity of Z_ℓ comes from quadrangulations leading to well-labeled 1-trees with a generic backbone and, moreover, with a marked vertex with label ℓ lying outside their skeleton. The shortest path in the 1-tree from the marked vertex to the skeleton defines a chain whose endpoint on the skeleton has label, say ℓ_3, and is generically different from the two vertices of degree 3 in the skeleton, with labels ℓ_1 and ℓ_2. The dominant singularity of Z_ℓ is therefore that of the "diagram" of fig. 7, whose value is obtained by replacing each edge by the corresponding propagator K and by summing over ℓ_1, ℓ_2 and ℓ_3, keeping ℓ fixed, namely

$$\sum_{\ell_1 \geq 1} \sum_{\ell_2 \geq 1} \sum_{\ell_3 \geq 1} K_{\ell,\ell_3} K_{\ell_1,\ell_3} K_{\ell_2,\ell_3} \left(K_{\ell_1,\ell_2}\right)^2 \ . \tag{5.1}$$

Setting $\ell = L/\sqrt{\epsilon}$ and turning to rescaled variables in the sums, we get a dominant singularity

$$\begin{aligned} Z_\ell &\sim \frac{1}{\epsilon^4}\int_0^\infty dL_1 \int_0^\infty dL_2 \int_0^\infty dL_3 \; \rho(L,L_3)\rho(L_1,L_3)\rho(L_2,L_3)\left(\rho(L_1,L_2)\right)^2 \\ &= \frac{\mathcal{F}^{(1)}(L)}{\epsilon^4} \end{aligned} \tag{5.2}$$

with a new scaling function $\mathcal{F}^{(1)}(L)$ which fully characterizes the two-point distance statistics in large toroidal maps. The above integrals can be performed explicitly and involve 12 sectors for the determination of the minimum in the formula (2.18) for ρ (2 relative positions for L and L_3 $\times$ 6 relative positions for L_1, L_2 and L_3), reducible by symmetry $L_1 \leftrightarrow L_2$ to 6 sectors. After some cumbersome but straightforward calculations, we find the relatively simple expression

$$\begin{aligned} \mathcal{F}^{(1)}(L) &= \mathcal{A}_0(L) + L\,\mathcal{A}_1(L) + L^2\mathcal{A}_2(L) \\ \text{with}\quad \mathcal{A}_0(L) &= \frac{1}{768}\frac{238 + 151\cosh(\sqrt{6}L) + \cosh(2\sqrt{6}L)}{\sinh^4\left(\sqrt{\frac{3}{2}}L\right)} \\ \mathcal{A}_1(L) &= -\frac{5}{2048\sqrt{6}}\frac{100\sinh(\sqrt{6}L) + 31\sinh(2\sqrt{6}L)}{\sinh^6\left(\sqrt{\frac{3}{2}}L\right)} \\ \mathcal{A}_2(L) &= -\frac{75}{1024}\frac{3 + 2\cosh(\sqrt{6}L)}{\sinh^6\left(\sqrt{\frac{3}{2}}L\right)}\ . \end{aligned} \tag{5.3}$$

This explicit formula constitutes the main result of this paper, with $\mathcal{F}^{(1)}$ playing for the toroidal topology the same role as $\mathcal{F}$ for the spherical case. It is worth noting that, from their explicit expressions, the three functions $\mathcal{A}_0$, $\mathcal{A}_1$ and $\mathcal{A}_2$, satisfy the remarkable relation

$$\mathcal{A}_0'' - 4\mathcal{A}_1' + 20\mathcal{A}_2 = 0 \tag{5.4}$$

so that we may write in all generality the parametrization

$$\mathcal{A}_0 = 4\alpha_0\ , \quad \mathcal{A}_1 = \alpha_0' + 5\alpha_1\ , \quad \mathcal{A}_2 = \alpha_1'\ . \tag{5.5}$$

In other words, the scaling function $\mathcal{F}^{(1)}$ may be written as

$$\begin{aligned} \mathcal{F}^{(1)}(L) &= 4\mathcal{M}(L) + L\mathcal{M}'(L) \\ \text{with } \mathcal{M}(L) &= \alpha_0(L) + L\alpha_1(L) \end{aligned} \tag{5.6}$$

in terms of a simpler function $\mathcal{M}$. We have no explanation for this particular form nor for the meaning of $\mathcal{M}(L)$ itself. From (5.3), we have explicitly

$$\begin{aligned}\alpha_0(L) &= \frac{1}{3072}\frac{238+151\cosh(\sqrt{6}L)+\cosh(2\sqrt{6}L)}{\sinh^4\left(\sqrt{\frac{3}{2}}L\right)}\\ \alpha_1(L) &= \frac{25}{512}\sqrt{\frac{3}{2}}\frac{\cosh\left(\sqrt{\frac{3}{2}}L\right)}{\sinh^5\left(\sqrt{\frac{3}{2}}L\right)}\ .\end{aligned} \tag{5.7}$$

At small L, although $\mathcal{A}_0$, $\mathcal{A}_1$ and $\mathcal{A}_2$ diverge respectively as $1/L^4$, $1/L^5$ and $1/L^6$, a number of cancellations ensure that $\mathcal{F}^{(1)}(L)$ vanishes as

$$\mathcal{F}^{(1)}(L) \sim \frac{L^4}{896}\ . \tag{5.8}$$

We deduce from this formula that for a large, but *finite* ℓ, i.e. in the so-called *local limit*, we have

$$Z_\ell \sim \frac{L^4}{896\epsilon^4} = \frac{\ell^4}{896\epsilon^2} \quad \text{and therefore} \quad Z_\ell|_{g^n} \sim \frac{12^n}{896}\ \ell^4 \tag{5.9}$$

at large n. Normalizing by the number $Q_\bullet^{(1)}|_{g^n} \sim 12^n/96$ of pointed quadrangulations, we find that the *average number* $\langle V_\ell\rangle_\bullet^{(1)}$ *of vertices* at a distance less than or equal to ℓ of the origin in pointed bipartite quadrangulations of genus 1 behaves, for large but finite ℓ, as

$$\langle V_\ell\rangle_\bullet^{(1)} \sim \frac{3}{28}\ell^4\ . \tag{5.10}$$

This is exactly the result found for planar quadrangulations, i.e. in the spherical case $h = 0$. As might be expected, the local limit is totally insensitive to the genus. The presence of handles may generically be felt only by traveling along distances of order $n^{1/4}$ in the map.

Alternatively, we may consider the scaling limit of pointed bipartite quadrangulations of genus 1 with fixed, large size n, but now with $\ell \propto n^{1/4}$. The probability $\Phi^{(1)}(r)$ that a vertex picked uniformly at random in the quadrangulation be at a distance less than $\ell = rn^{1/4}$ from the origin is given by

$$\begin{aligned}\Phi^{(1)}(r) &= \frac{96}{\pi}\int_{-\infty}^{\infty} d\xi\ \frac{1}{\mathrm{i}\xi^3}\exp(-\xi^2)\mathcal{F}^{(1)}(\sqrt{-\mathrm{i}\xi}\,r)\\ &= \frac{3\,r^4}{28} + \frac{96}{\pi}\int_{-\infty}^{\infty} d\xi\ \frac{1}{\mathrm{i}\xi^3}\exp(-\xi^2)\left(\mathcal{F}^{(1)}(\sqrt{-\mathrm{i}\xi}\,r) - \frac{(\sqrt{-\mathrm{i}\xi}\,r)^4}{896}\right)\\ &= \frac{3\,r^4}{28} + \frac{96}{\pi}\int_{0}^{\infty} d\xi\ \frac{1}{\mathrm{i}\xi^3}\exp(-\xi^2)\left(\mathcal{F}^{(1)}(\sqrt{-\mathrm{i}\xi}\,r) - \mathcal{F}^{(1)}(\sqrt{\mathrm{i}\xi}\,r)\right)\end{aligned} \tag{5.11}$$

where we singled out the contribution from the first term in the small r expansion of $\mathcal{F}^{(1)}(r)$, corresponding precisely to the local limit, as it is proportional to the improper

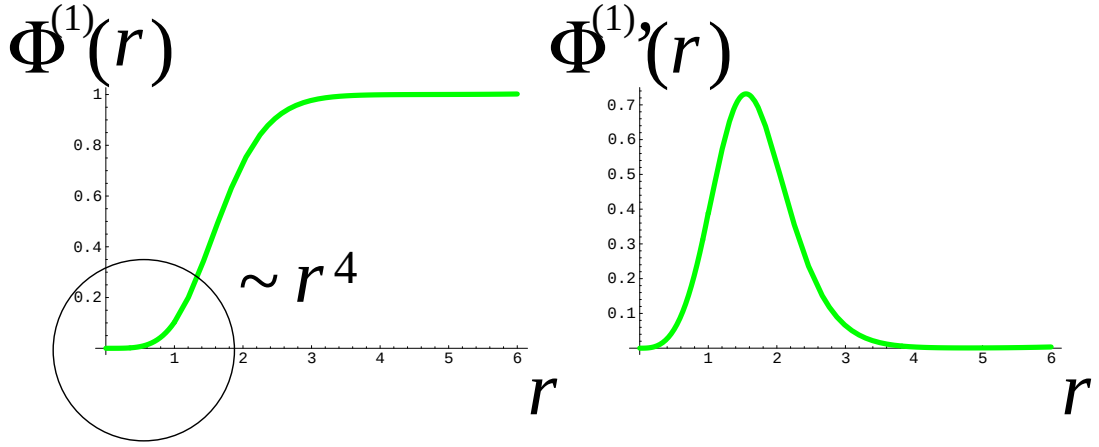

Fig. 8: Plots of the cumulative probability distribution $\Phi^{(1)}(r)$ and the associated probability density $\Phi^{(1)\prime}(r)$ for the rescaled distance r from a uniformly chosen random vertex to the origin of a large pointed toroidal quadrangulation.

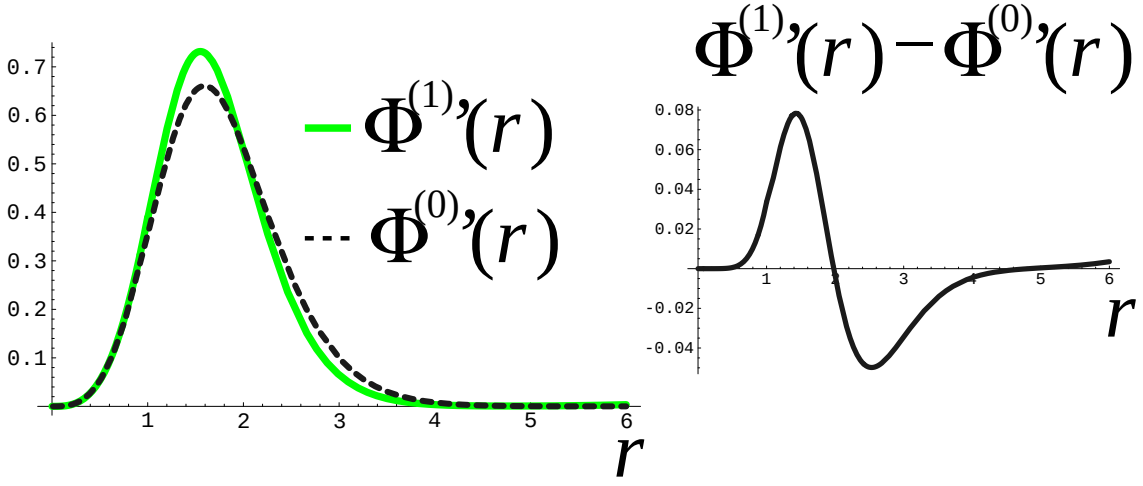

Fig. 9: Comparison of the probability densities $\Phi^{(1)\prime}(r)$ and $\Phi^{(0)\prime}(r)$ for the rescaled distance r from a uniformly chosen random vertex to the origin in large pointed toroidal and planar quadrangulations respectively. We plotted on the right the difference $\Phi^{(1)\prime} - \Phi^{(0)\prime}$.

integral $\int_{-\infty}^{\infty}(d\xi/\xi)\exp(-\xi^2)$. Its value $-\mathrm{i}\pi$ of this integral is dictated by the change of variable from g to ξ. The integrals in the second and third lines of (5.11) are now convergent integrals. Expanding further at small r gives

$$\Phi^{(1)}(r) = \frac{3r^4}{28} - \frac{15r^{10}}{1456\sqrt{\pi}} + \frac{1242135r^{14}}{506970464\sqrt{\pi}} + \mathcal{O}\left(r^{18}\right) \tag{5.12}$$

with, as discussed above, the same leading term $\propto r^4$ as for planar quadrangulations, but now a first negative correction of order r^{10} instead of r^8 for the planar two-point function.

The two-point function therefore increases faster at small r for toroidal maps than for spherical ones. The probability distribution $\Phi^{(1)}(r)$ and the associated probability density $\Phi^{(1)\prime}(r)$ are plotted in fig. 8. A comparison with the corresponding genus 0 probability density $\Phi^{(0)\prime}(r)$, as computed in ref. [17], is displayed in fig. 9.

6. Conclusion

In this paper, we have derived explicit expressions for a number of probability distributions characterizing the distance statistics of large toroidal maps. These distributions, obtained here in the context of bipartite quadrangulations, are expected to be universal (up to a non-universal global rescaling of r) and describe the distance statistics in more general ensembles of large toroidal maps in the universality class of pure gravity, such has maps with prescribed face degrees, possibly equipped with non-critical statistical models.

Our main result is the explicit form (5.3) for the two-point scaling function $\mathcal{F}^{(1)}$, which is the genus 1 counterpart of spherical two-point scaling function $\mathcal{F}$ of eq. (2.5). In the same way as $\mathcal{F}$ satisfies the non-linear differential equation (2.6), we may wonder if $\mathcal{F}^{(1)}$ itself obeys some simple differential equation, possibly involving $\mathcal{F}$ as a source. Our method, which consisted in a direct computation of $\mathcal{F}^{(1)}$, did not allow us to find such an equation.

Among possible extensions of our work, let us mention the computation of the toroidal three-point function or more simply, that of a more involved two-point function now measuring the "second-shortest length between two points", i.e. the length of any shortest path among those paths not homotopic to the true geodesic. There seems to be no fundamental obstacle to the derivation of these laws but the calculations may rapidly become heavy.

Another natural extension if of course that of maps with genus $h > 1$. Here a more fundamental obstacle occurs since, when h becomes large, we have to deal with a large number of diagrams, each involving a large number of propagators, which makes in practice our method unadapted. Alternatively, one may hope for the existence of a hierarchy of equations satisfied by the higher genus two-point functions, whose discovery would be a promising step in the quest for these universal scaling functions.

References

[1] W. Tutte, *A Census of planar triangulations* Canad. J. of Math. **14** (1962) 21-38; *A Census of Hamiltonian polygons* Canad. J. of Math. **14** (1962) 402-417; *A Census of slicings*, Canad. J. of Math. **14** (1962) 708-722; *A Census of Planar Maps*, Canad. J. of Math. **15** (1963) 249-271.

[2] E. Brézin, C. Itzykson, G. Parisi and J.-B. Zuber, *Planar Diagrams*, Comm. Math. Phys. **59** (1978) 35-51.

[3] P. Di Francesco, *2D Quantum Gravity, Matrix Models and Graph Combinatorics*, Lecture notes given at the summer school "Applications of random matrices to physics", Les Houches, June 2004, arXiv:math-ph/0406013.

[4] R. Cori and B. Vauquelin, *Planar maps are well labeled trees*, Canad. J. Math. **33(5)** (1981) 1023-1042.

[5] G. Schaeffer, *Conjugaison d'arbres et cartes combinatoires aléatoires*, PhD Thesis, Université Bordeaux I (1998).

[6] J. Bouttier, P. Di Francesco and E. Guitter. *Planar maps as labeled mobiles*, Elec. Jour. of Combinatorics **11** (2004) R69, arXiv:math.CO/0405099.

[7] V. Kazakov, *Bilocal regularization of models of random surfaces*, Phys. Lett. **B150** (1985) 282-284; F. David, *Planar diagrams, two-dimensional lattice gravity and surface models*, Nucl. Phys. **B257** (1985) 45-58; J. Ambjørn, B. Durhuus and J. Fröhlich, *Diseases of triangulated random surface models and possible cures*, Nucl. Phys. **B257** (1985) 433-449; V. Kazakov, I. Kostov and A. Migdal *Critical properties of randomly triangulated planar random surfaces*, Phys. Lett. **B157** (1985) 295-300.

[8] for a review, see: P. Di Francesco, P. Ginsparg and J. Zinn–Justin, *2D Gravity and Random Matrices*, Physics Reports **254** (1995) 1-131.

[9] J. F. Marckert and A. Mokkadem, *Limit of normalized quadrangulations: the Brownian map*, Annals of Probability **34(6)** (2006) 2144-2202, arXiv:math.PR/0403398.

[10] J. F. Le Gall, *The topological structure of scaling limits of large planar maps*, invent. math. **169** (2007) 621-670, arXiv:math.PR/0607567.

[11] J. F. Le Gall and F. Paulin, *Scaling limits of bipartite planar maps are homeomorphic to the 2-sphere*, Geomet. Funct. Anal. **18**, 893-918 (2008), arXiv:math.PR/0612315.

[12] G. Miermont, *On the sphericity of scaling limits of random planar quadrangulations*, Elect. Comm. Probab. **13** (2008) 248-257, arXiv:0712.3687 [math.PR].

[13] J.-F. Le Gall, *Geodesics in large planar maps and in the Brownian map*, Acta Math., to appear, arXiv:0804.3012 [math.PR].

[14] J. Ambjørn and Y. Watabiki, *Scaling in quantum gravity*, Nucl.Phys. **B445** (1995) 129-144, arXiv:hep-th/9501049.

[15] J. Ambjørn, J. Jurkiewicz and Y. Watabiki, *On the fractal structure of two-dimensional quantum gravity*, Nucl.Phys. **B454** (1995) 313-342, arXiv:hep-lat/9507014.

[16] see also J. Ambjørn, B. Durhuus and T. Jonsson, *Quantum Geometry: A statistical field theory approach*, Cambridge University Press, 1997.

[17] J. Bouttier, P. Di Francesco and E. Guitter, *Geodesic distance in planar graphs*, Nucl. Phys. **B663**[FS] (2003) 535-567, arXiv:cond-mat/0303272.

[18] J. Bouttier and E. Guitter, *The three-point function of planar quadrangulations*, J. Stat. Mech. (2008) P07020, arXiv:0805.2355 [math-ph].

[19] J. Bouttier and E. Guitter, *Confluence of geodesic paths and separating loops in large planar quadrangulations*, J. Stat. Mech. (2009) P03001, arXiv:0811.0509 [math-ph].

[20] J. Bouttier and E. Guitter *Distance statistics in quadrangulations with a boundary, or with a self-avoiding loop*, J. Phys. A: Math. Theor. **42** (2009) 465208, arXiv:0906.4892 [math-ph].

[21] M. Marcus and G. Schaeffer, *Une bijection simple pour les cartes orientables* (2001), available at http://www.lix.polytechnique.fr/Labo/Gilles.Schaeffer/Biblio/.

[22] see also G. Chapuy, M. Marcus and G. Schaeffer, *A bijection for rooted maps on orientable surfaces*, SIAM J. Discrete Math. **23**(3) (2009) 1587-1611, arXiv:0712.3649 [math.CO].

[23] J. Bettinelli, *Scaling Limits for Random Quadrangulations of Positive Genus*, preprint arXiv:1002.3682 [math.PR].

[24] T. Jonsson, *Width of handles in two-dimensional quantum gravity*, Phys. Lett. **B 425** (1998) 265-268, arXiv:hep-th/9801150.